





# Prion-like $\alpha$ -synuclein pathology in the brain of infants with Krabbe disease

Christopher Hatton,<sup>1,2</sup> Simona S. Ghanem,<sup>3</sup>  David J. Koss,<sup>2</sup> Ilham Y. Abdi,<sup>3</sup> Elizabeth Gibbons,<sup>4</sup> Rita Guerreiro,<sup>4,5</sup> Jose Bras,<sup>4,5</sup> International DLB Genetics Consortium, Lauren Walker,<sup>2</sup> Ellen Gelpi,<sup>6</sup> Wendy Heywood,<sup>7</sup> Tiago F. Outeiro,<sup>2,8,9,10</sup> Johannes Attems,<sup>2</sup> Robert McFarland,<sup>1,2,11</sup> Rob Forsyth,<sup>2,11</sup> Omar M. El-Agnaf<sup>3</sup> and  Daniel Erskine<sup>1,2</sup>

See Kwatra *et al.* (<https://doi.org/10.1093/brain/awac108>) for a scientific commentary on this article.

Krabbe disease is an infantile neurodegenerative disorder resulting from pathogenic variants in the *GALC* gene that causes accumulation of the toxic sphingolipid psychosine. *GALC* variants are also associated with Lewy body diseases, an umbrella term for age-associated neurodegenerative diseases in which the protein  $\alpha$ -synuclein aggregates into Lewy bodies. To explore whether  $\alpha$ -synuclein in Krabbe disease has pathological similarities to that in Lewy body disease, we performed an observational post-mortem study of Krabbe disease brain tissue ( $n = 4$ ) compared to infant controls ( $n = 4$ ) and identified widespread accumulations of  $\alpha$ -synuclein. To determine whether  $\alpha$ -synuclein in Krabbe disease brain displayed disease-associated pathogenic properties we evaluated its seeding capacity using the real-time quaking-induced conversion assay in two cases for which frozen tissue was available and strikingly identified aggregation into fibrils similar to those observed in Lewy body disease, confirming the prion-like capacity of Krabbe disease-derived  $\alpha$ -synuclein. These observations constitute the first report of prion-like  $\alpha$ -synuclein in the brain tissue of infants and challenge the putative view that  $\alpha$ -synuclein pathology is merely an age-associated phenomenon, instead suggesting it results from alterations to biological pathways, such as sphingolipid metabolism. Our findings have important implications for understanding the mechanisms underlying Lewy body formation in Lewy body disease.

- 1 Wellcome Centre for Mitochondrial Research, Claremont Road, Newcastle NE2 4AA, UK
- 2 Translational and Clinical Research Institute, Newcastle University, Newcastle NE2 4AA, UK
- 3 Neurological Disorders Research Center, Qatar Biomedical Research Institute (QBRI), Hamad Bin Khalifa University (HBKU), Qatar Foundation, Doha 34110, Qatar
- 4 Department of Neurodegenerative Science, Van Andel Institute, Grand Rapids, MI 49503, USA
- 5 Division of Psychiatry and Behavioral Medicine, Michigan State University College of Human Medicine, Grand Rapids, MI 49503, USA
- 6 Division of Neuropathology and Neurochemistry, Department of Neurology, Medical University of Vienna, 1090 Vienna, Austria
- 7 UCL Great Ormond Street Institute of Child Health, London WC1N 1EH, UK
- 8 Department of Experimental Neurodegeneration, Center for Biostructural Imaging of Neurodegeneration, University Medical Center Göttingen, 37073 Göttingen, Germany
- 9 Max Planck Institute for Experimental Medicine, 37075 Göttingen, Germany
- 10 Scientific employee with an honorary contract at Deutsches Zentrum für Neurodegenerative Erkrankungen (DZNE), 37075 Göttingen, Germany
- 11 Department of Paediatric Neurology, Great North Children's Hospital, Newcastle NE1 4LP, UK

Received October 20, 2021. Revised November 22, 2021. Accepted December 10, 2021. Advance access publication January 6, 2022

© The Author(s) 2022. Published by Oxford University Press on behalf of the Guarantors of Brain.

This is an Open Access article distributed under the terms of the Creative Commons Attribution-NonCommercial License (<https://creativecommons.org/licenses/by-nc/4.0/>), which permits non-commercial re-use, distribution, and reproduction in any medium, provided the original work is properly cited. For commercial re-use, please contact [journals.permissions@oup.com](mailto:journals.permissions@oup.com)

Correspondence to: Dr Daniel Erskine  
Wellcome Centre for Mitochondrial Research  
Newcastle University, Claremont Place  
Newcastle upon Tyne, NE2 4AA, UK  
E-mail: daniel.erskine@ncl.ac.uk

**Keywords:** Krabbe disease; Lewy body disease;  $\alpha$ -synuclein; sphingolipids

**Abbreviations:** DLB = dementia with Lewy bodies; LBD = Lewy body dementia; RT-QuIC = real-time quaking-induced conversion

## Introduction

Krabbe disease is a rare autosomal recessive neurodegenerative disorder caused by mutations in the *GALC* gene that encodes the lysosomal enzyme  $\beta$ -galactocerebrosidase and usually presents within the first months of life and typically leads to death by the age of 2 years old.<sup>1</sup> Loss of  $\beta$ -galactocerebrosidase activity leads to accumulation of the cytotoxic sphingolipid psychosine/galactosyl-sphingosine and associated oligodendroglial loss underlying the striking leukodystrophy that characterizes this condition.

In contrast to the infantile onset of Krabbe disease, Lewy body diseases (LBD), such as Parkinson's disease and dementia with Lewy bodies (DLB), are associated with advancing age and are characterized by the aggregation of the protein  $\alpha$ -synuclein, which is thought to be central to the pathogenesis of these disorders.<sup>2</sup> In addition to causing Krabbe disease, *GALC* is also associated with risk of sporadic Parkinson's disease and psychosine has been demonstrated to promote the aggregation of  $\alpha$ -synuclein into forms associated with LBD.<sup>3,4</sup> Previous studies have reported  $\alpha$ -synuclein accumulations in Krabbe disease frontal cortex and spinal cord neurons.<sup>5,6</sup> As we have previously noted,  $\alpha$ -synuclein is reported to accumulate in a number of neurometabolic diseases, although as most studies have only used pan- $\alpha$ -synuclein antibodies it is not clear whether such accumulations have putative pathogenic modifications associated with LBD, such as phosphorylation at serine 129 (pS129) or seed-competence, limiting inference of shared mechanisms.<sup>7,8</sup> To address this knowledge gap, we performed an observational cross-sectional study of Krabbe disease brain tissue and hypothesized that it would contain deposits of  $\alpha$ -synuclein with prion-like attributes.

## Materials and methods

### Post-mortem tissue preparation

Cases were included based on availability and prepared according to standard brain banking protocols ([Supplementary material](#)). Newcastle Brain Tissue Resource Ethics Committee granted ethical approval for KD1, KD3, the DLB case and all control cases ([Table 1](#)), while approval for the study and cases KD2 and KD4 was granted by Newcastle University Ethical Review Board (14201/2020). Immunohistochemical and fluorescent protocols are described in the [Supplementary material](#).

### Sodium dodecyl sulphate–polyacrylamide gel electrophoresis and western blot analysis

Frozen tissue for sodium dodecyl sulphate–polyacrylamide gel electrophoresis and western blot was prepared as described in [Supplementary material](#). Protein titres were normalized across samples using the Bradford assay (Thermo Scientific). Samples were mixed with lithium dodecyl sulphate (NuPage, Thermo Scientific) and dithiothreitol (15 mM dithiothreitol, Sigma) before

boiling at 70°C for 10 min. Samples (10  $\mu$ g/lane) were separated on 4–12% Bis-Tris gels in MOPS buffer and electroblotted onto 0.45- $\mu$ m nitrocellulose membranes (iBlot 2, NuPage, Thermo Scientific). PageRuler Plus prestained protein ladders (3  $\mu$ g/lane) were included as a protein molecular weight standard.

$\alpha$ -Synuclein was fixed to membranes by boiling for 10 min in PBS before membranes were washed in Tris-buffered saline containing 0.05% Tween 20 (TBST, in mM; 50 Trizma base, 150 NaCl, pH = 7.6) and blocked for 1 h at room temperature in 5% bovine serum albumin in TBST before overnight incubation at 4°C with primary antibodies ([Supplementary Table 2](#)). Antibody binding was visualized with secondary antibodies ([Supplementary Table 2](#)) conjugated to horseradish peroxidase and chemiluminescence using 1.25 mM luminol, 30  $\mu$ M coumaric acid and 0.0015% hydrogen peroxide. Membranes were visualized on a Fuji LAS4000 (Fuji LAS Image, Raytek) and equal loading across lanes was confirmed via staining with Ponceau S (Sigma). The primary aim of this aspect of the study was to identify whether high molecular weight  $\alpha$ -synuclein would be found in Krabbe disease cases compared to controls.

### RT-QuIC assay

Expression and purification of recombinant full-length  $\alpha$ -synuclein and preparation of brain samples for real-time quaking-induced conversion assay (RT-QuIC) was performed as previously ([Supplementary material](#)).<sup>9</sup> Frozen brain tissue lysates were used from Cases KD1 and KD3 and from four infant control cases based on tissue availability.

The RT-QuIC reaction buffer was 100 mM piperazine-N, N'-bis(ethanesulfonic acid) (pH 6.9), 0.1 mg/ml  $\alpha$ Syn and 10  $\mu$ M Thioflavin-T. Reactions were performed in triplicate in black 96-well plates with a clear bottom (Nunc, Thermo Fisher) with 85  $\mu$ l of the reaction mix loaded into each well together with 15  $\mu$ l of 0.1 mg/ml TBS-soluble or detergent-soluble fractions. The plate was then sealed with a sealing film (Thermo Fisher) and incubated in a BMG LABTECH FLUOstar OMEGA plate reader at 37°C for 100 h with intermittent cycles of 1 min of shaking (500 rpm, double orbital) and 15 min of rest throughout the indicated incubation time. Thioflavin-T fluorescence measurements, expressed as arbitrary relative fluorescence units, were taken with bottom reads every 15 min using 450  $\pm$  10 nm (excitation) and 480  $\pm$  10 nm (emission) wavelengths for 80 h and a positive signal was defined as relative fluorescence units >5 standard deviation units above the mean of initial fluorescence, as previously.<sup>10</sup> The sample was considered positive if all of the replicates were positive, otherwise the sample was classified as negative. RT-QuIC was performed twice to confirm positive results.

For electron microscopy to confirm the presence of fibrils, RT-QuIC end-products were transferred in a 5  $\mu$ l volume to a transmission electron microscopy grid (S162 Formvar/Carbon, 200 Mesh, agar scientific). After 1 min, samples were fixed using 5  $\mu$ l of 0.5% glutaraldehyde followed by one wash with 50  $\mu$ l of deionized water. Then 5  $\mu$ l of 2% uranyl acetate were added to the grid, and after

Table 1 Demographic details of the cohort

Case ID	Sex	Diagnosis	Presentation	Disease duration	Age at death	Brain weight, g
KD1	Male	KD	Failure to thrive and developmental delay at 6 months, later developed frequent apnoea and vomiting, spastic quadriplegia, microcephaly and visual loss. Diagnosis by clinical impression and later confirmed by post-mortem demonstration of absent galactocerebrosidase activity in cortex.	4 months	10 months	660
KD2	Male	KD	Central hypotonia and head lag at 4 months, developmental delay and persistent crying noted at 5.5 months and later developed seizure-like activity. Diagnosis confirmed by reduced galactocerebrosidase activity.	6 months	10 months	ND
KD3	Female	KD	Status epilepticus following chest infection at 2 months, followed by developmental delay and feeding difficulties. Later developed central hypotonia and spasticity, then epileptic encephalopathy. Diagnosis confirmed by reduced galactocerebrosidase activity and genetic testing indicated homozygous 30-kb deletion in exons 11 through 17 of GALC gene.	10 months	12 months	690
KD4	Male	KD	Following vaccination at 5 months developed enteritis followed by restlessness and crying, followed by spastic tetraplegia, opisthotonos, apnoea and continuous crying. Later developed generalized myoclonus, aspiration episodes, bradycardia and pneumonia, against backdrop of progressive failure to thrive. Diagnosis was made by neuropathological examination but a sibling later demonstrated reduced galactocerebrosidase activity.	10 months	15 months	730
C1	Male	SIDS	Parent awoke to find infant unresponsive in their arms, pronounced dead on arrival at hospital. SIDS diagnosed due to absence of obvious cause of death on post-mortem examination.	NA	3 months	640
C2	Male	Hypoxic-ischaemic encephalopathy	Hypoxia-ischaemia due to prolonged labour, died after 1 month in the Special Care Baby Unit.	1 months	1 months	ND
C3	Female	SIDS	Parents discovered deceased in bed. SIDS diagnosed due to absence of obvious cause of death on post-mortem examination.	NA	20 months	ND
C4	Male	SIDS	Parents discovered deceased in cot. SIDS diagnosed due to absence of obvious cause of death on post-mortem examination.	NA	2 months	570
DLB	Male	DLB	Presented with visual hallucinations and cognitive fluctuations, diagnosed with DLB.	4 years	81 years	1331

C = control; KD = Krabbe disease; NA = not applicable; ND = not determined; SIDS = sudden infant death syndrome.

2 min uranyl acetate was blotted off and grids were dried before placing sample holders before visualization.

### Association of GALC variants with DLB

To determine whether GALC is associated with risk of DLB, we analysed existing cohorts collected as part of the International DLB Genetics Consortium. Details of analyses performed can be found in the [Supplementary material](#).

### Data availability

Data are available from the corresponding author on reasonable request.

## Results

### $\alpha$ -Synuclein is abnormally expressed in Krabbe disease

Using the pan- $\alpha$ -synuclein antibody Syn1 and the autophagic marker p62/SQSTM1, we did not observe Lewy body pathology in any case. However, we identified  $\alpha$ -synuclein to be variably present within globoid cells, multi-nucleated white matter macrophages that are the characteristic neuropathological feature of Krabbe disease, and this was particularly marked in the medulla oblongata,

crus cerebri and cerebral cortex (Fig. 1A and [Supplementary Fig. 1](#)). Globoid cells were rarely immunoreactive for the autophagic marker p62/SQSTM1, the accumulation of which may indicate accumulated cellular waste (Fig. 1B and C). To determine whether  $\alpha$ -synuclein in globoid cells was immunoreactive for  $\alpha$ -synuclein modifications associated with LBD, we stained sections with the conformation-specific  $\alpha$ -synuclein antibodies Syn-O2 and 5G4, and  $\alpha$ -synuclein pS129, all of which are associated with LBD, but did not observe globoid cells labelled.<sup>2,11,12</sup>

In the cortex of Krabbe disease cases, we noted a sub-population of deep layer cortical pyramidal neurons that were labelled by Syn1 but not p62/SQSTM1 (Fig. 1D). Although  $\alpha$ -synuclein labels some pyramidal neurons in the developing brain up until the age of 12 months ([Supplementary Fig. 2](#)), neuronal  $\alpha$ -synuclein was notably present in both Krabbe disease cases aged over 12 months.<sup>13</sup> To study this population of neurons further while controlling for differences in  $\alpha$ -synuclein expression in the developing brain, we compared Krabbe disease temporal cortex tissue to that from infant controls ([Supplementary Table 1](#)). We noted some Krabbe disease pyramidal neurons, again typically in deep cortical layers, that were strongly immunoreactive for the  $\alpha$ -synuclein oligomer marker Syn-O2, lightly labelled for the  $\alpha$ -synuclein aggregate-specific marker 5G4 but not labelled by pS129 (Fig. 1E and F and [Supplementary Fig. 1](#)) and this differed from infant control cases ([Supplementary Fig. 2](#)). It is possible that the currently reported



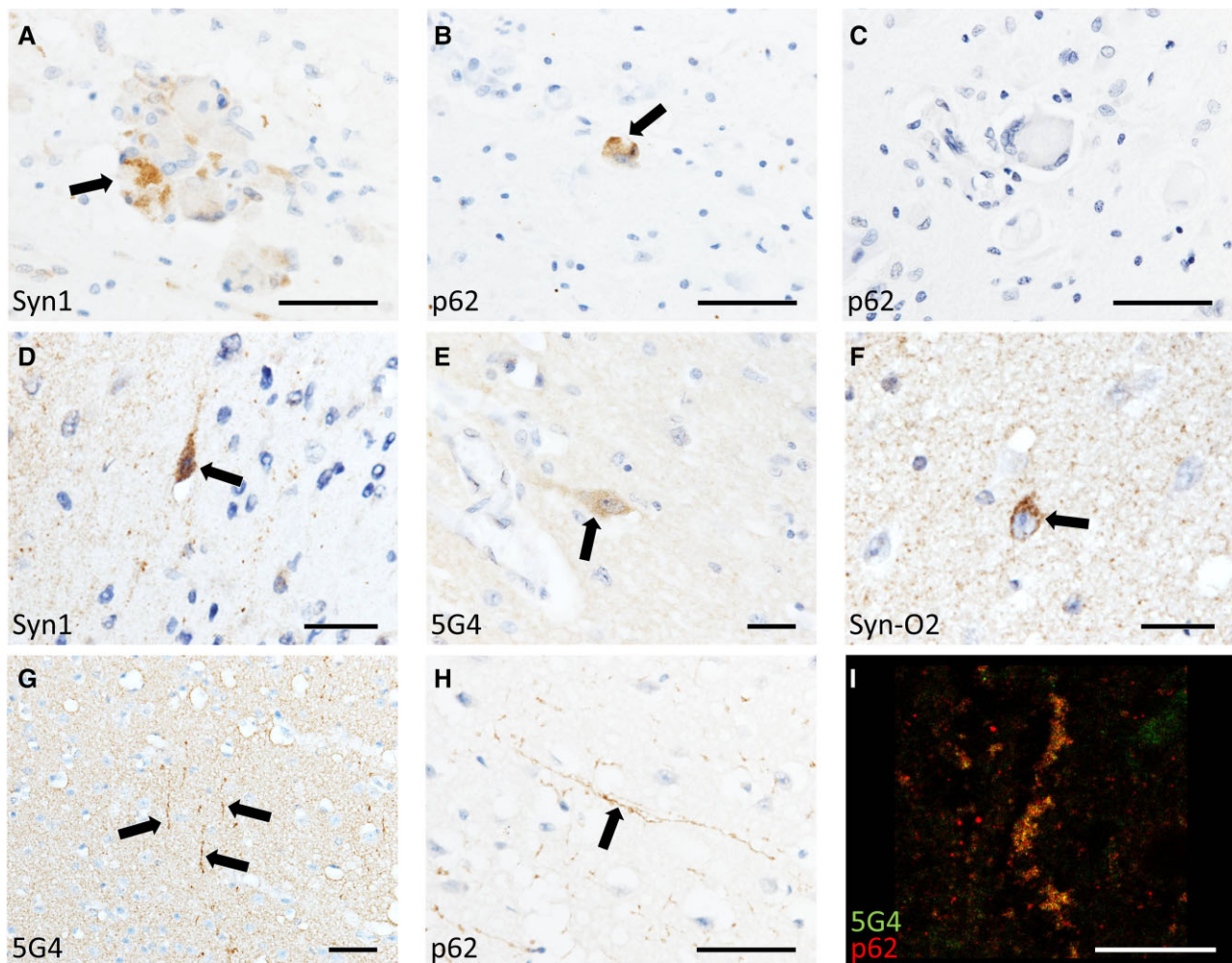


**Figure 1**  $\alpha$ -Synuclein in Krabbe disease. Photomicrographs of Krabbe disease (KD) cases demonstrating  $\alpha$ -synuclein-immunoreactive globoid cells (A) that were variably positive for the autophagic marker p62 (B and C). Occasional neurons manifested punctate  $\alpha$ -synuclein staining (D–F) and neurites that were immunoreactive for  $\alpha$ -synuclein and p62 were variably present throughout the cortex of all cases (GI). Scale bars = 50  $\mu$ m (A–C, G and H) 25  $\mu$ m (D–F) and 20  $\mu$ m (I).

$\alpha$ -synuclein immunoreactivity in neurons correspond with the amorphous intraneuronal aggregates previously reported in Krabbe disease brain tissue.<sup>6</sup> We also observed long cortical neurites that were immunoreactive for p62/SQSTM1 and 5G4 (Fig. 1G–I and Supplementary Fig. 1), but these were not labelled by Syn1, Syn-O2 or pS129.

### Immunoblotting of Krabbe disease brain lysates demonstrates dysregulated $\alpha$ -synuclein

To explore the nature of  $\alpha$ -synuclein changes in Krabbe disease we performed immunoblotting on two cases for which frozen tissue was available (Cases KD1 and KD3) and compared these to four infant control cases and one LBD case as a synucleinopathy disease control (Supplementary Table 1). We selected temporal cortex as it manifested  $\alpha$ -synuclein pathology in both Krabbe disease cases and evaluated grey and white matter separately. We did not observe consistent changes in total  $\alpha$ -synuclein in Krabbe disease or the LBD case (Supplementary Fig. 3). However, dysregulated  $\alpha$ -synuclein was identified in both grey and white matter of Krabbe disease cases, as shown by higher molecular weight bands of pS129 at ~20 and 40 kDa that were remarkably similar in both Krabbe disease cases (Fig. 2A and B and

Supplementary Fig. 3). However, the higher molecular weight pS129 bands in Krabbe disease differed from those in the LBD case included as a disease control, suggesting that although  $\alpha$ -synuclein is dysregulated in Krabbe disease, it differs from that observed in LBD (Fig. 2A, B and Supplementary Figs 3 and 4).

### Krabbe disease brain lysates are seed-competent on RT-QuIC

A key pathogenic quality ascribed to  $\alpha$ -synuclein in LBD is its prion-like capacity, where a 'seed' of misfolded  $\alpha$ -synuclein can induce  $\alpha$ -synuclein monomers to misfold and aggregate into insoluble fibrils.<sup>2</sup> As psychosine, the cytotoxic sphingolipid that accumulates in Krabbe disease white matter, has been reported to induce  $\alpha$ -synuclein misfolding and aggregation *in vitro*, we hypothesized that  $\alpha$ -synuclein in Krabbe disease would have prion-like qualities and would therefore be capable of seeding monomeric  $\alpha$ -synuclein to misfold into fibrils.<sup>6</sup> We performed the real-time quaking-induced conversion (RT-QuIC) assay, where Krabbe disease temporal cortex samples were mixed with recombinant  $\alpha$ -synuclein and agitated, on the basis that if there is prion-like  $\alpha$ -synuclein within the tissues they will seed the aggregation of the recombinant protein into fibrils detectable by the amyloid dye Thioflavin-T.<sup>9</sup> RT-QuIC identified that

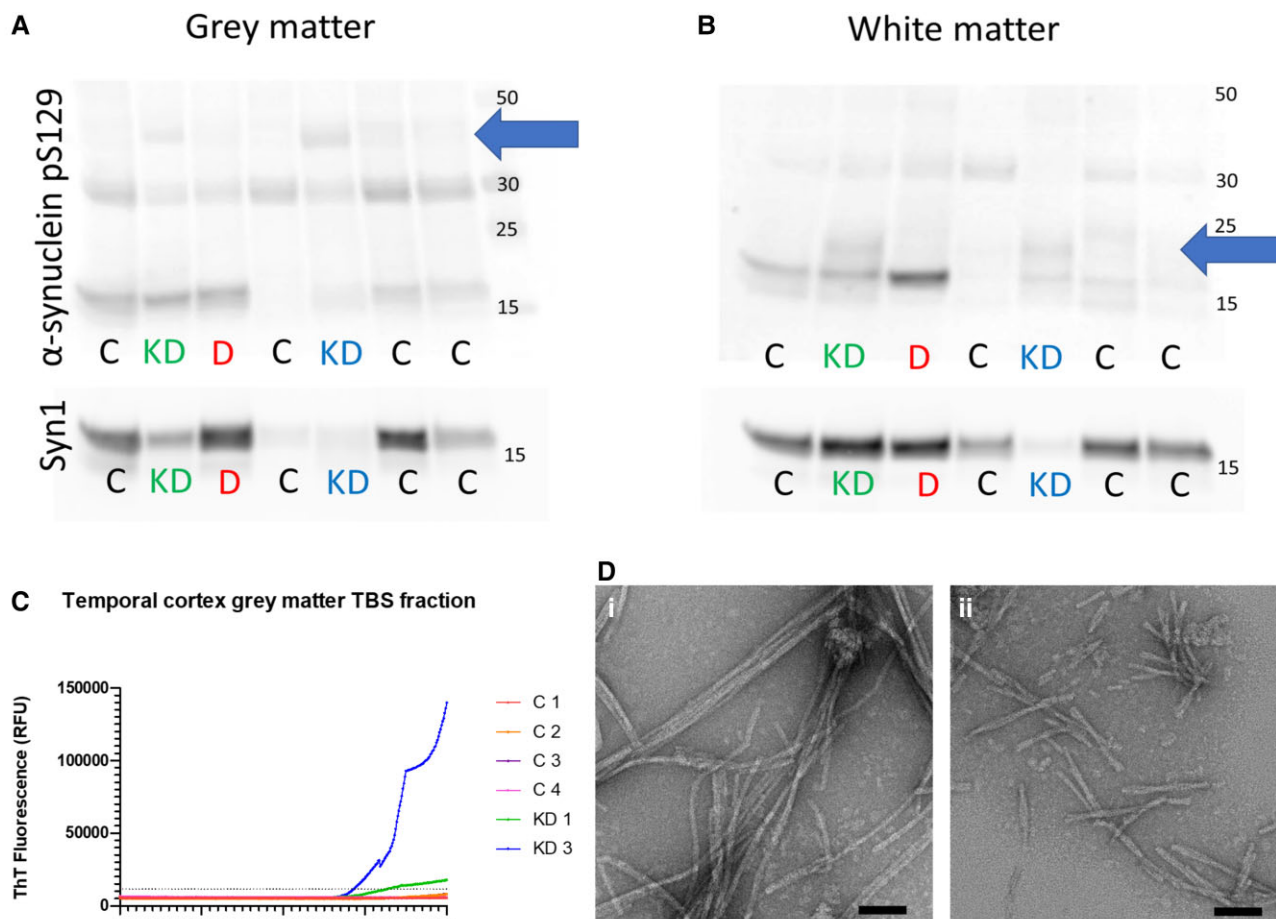


**Figure 2** Western blot and RT-QuIC of Krabbe disease brain tissue lysates. The TEAB-soluble fraction of KD temporal cortex grey matter lysates contained pS129 bands at ~40 kDa (blue arrow) that were not observed in control cases or the DLB case (A). In white matter samples, KD cases had additional bands of pS129 at ~20 kDa (blue arrow) that were not present in control or DLB cases (B). RT-QuIC of the TBS-soluble tissue fractions demonstrated that KD1 and KD3 grey matter gave positive reactions, defined as Thioflavin-T fluorescence >5 times the control standard deviation, at ~55 h while no reaction was observed in white matter samples (C). Transmission electron microscopy of RT-QuIC end-products from grey matter of KD1 [D(i)] and KD3 [D(ii)] confirmed the presence of fibrillar structures. It is notable that KD1 RT-QuIC end-products led to elongated fibrils of ~200–400 nm while KD3 end-products were typically 100–200 nm [E(i) and F(ii)]. Scale bars = 50 nm [D(i) and ii)].

the aqueous fraction of the grey matter of both Krabbe disease cases seeded aggregation into fibrils, indicating it has prion-like capacity (Fig. 2C), with similar intensity to LBD samples we have previously reported using the same assay.<sup>9</sup> In contrast, the detergent-soluble fraction of grey matter and both white matter tissue fractions did not give a positive RT-QuIC reaction (Supplementary Fig. 5). Transmission electron microscopy of RT-QuIC end-products from the aqueous fraction of grey matter from both Krabbe disease cases confirmed the presence of fibrils [Fig. 2D(i and ii)].

### GALC variants are not associated with DLB risk

Prion-like  $\alpha$ -synuclein is a feature of an age-associated disease,<sup>9</sup> thus its presence in infants with Krabbe disease probably indicates an association between altered sphingolipid metabolism and  $\alpha$ -synuclein aggregation that may be relevant to the pathogenesis of LBD. A previous meta-analysis using over 19 000 Parkinson's disease cases reported mutations in the GALC gene as a risk factor for Parkinson's disease, which prompted us to determine whether GALC variants are also associated with increased risk of DLB (Supplementary material).<sup>3</sup> However, our analysis using a smaller cohort of 2414 DLB cases from previous

studies did not identify GALC to be associated with DLB (Supplementary material).<sup>14,15</sup> We did identify two heterozygous missense variants that were potentially deleterious (Combined Annotation Dependent Depletion score >20) and only observed in DLB cases (Supplementary material). Given the much smaller cohort compared to that used to study GALC in Parkinson's disease, it is plausible that our study was less-powered to detect an association. DLB is also associated with significant levels of concomitant Alzheimer-type pathology that influences the clinical phenotype, making it a less pure disorder of  $\alpha$ -synuclein than Parkinson's disease.<sup>16,17</sup>

### Discussion

Despite occurring at opposite ends of the spectrum of age, Krabbe disease shares similarities as the GALC gene that causes Krabbe disease is also implicated in sporadic Parkinson's disease.<sup>3</sup> Furthermore, the protein  $\alpha$ -synuclein that is thought to underlie LBD pathogenesis has also been demonstrated to accumulate in Krabbe disease, although no study has yet determined whether  $\alpha$ -synuclein in Krabbe disease recapitulates key pathogenic qualities of  $\alpha$ -synuclein in LBD.<sup>6</sup> On this basis, we carried out a detailed examination of

$\alpha$ -synuclein from which we report, for the first time to our knowledge, the presence of  $\alpha$ -synuclein with prion-like characteristics in the brain tissue of infants.

The present findings challenge the putative view that  $\alpha$ -synuclein aggregation is merely an age-associated pathological alteration and instead suggests dysfunction of common biological pathways, such as sphingolipid metabolism, may underlie this phenomenon.<sup>2,18</sup> It is notable that psychosine has previously been reported as elevated in LBD brain tissue and in individuals carrying heterozygous GALC mutations, suggesting a direct link between psychosine metabolism and LBD.<sup>19</sup> Furthermore, the link between LBD and Krabbe disease processes may suggest that future drugs could be repurposed from LBD to Krabbe disease, including drugs that aim to attenuate  $\alpha$ -synuclein aggregation by ameliorating sphingolipid metabolism.

The time taken for  $\alpha$ -synuclein to develop into disease-relevant species is not currently known. However, the onset of non-motor symptoms such as disturbed sleep and altered sexual function ~5 years before motor symptoms and the presence of accumulated  $\alpha$ -synuclein in the colon up to 20 years before motor symptoms, may suggest a relatively long time period for  $\alpha$ -synuclein to develop into pathogenic forms.<sup>20–22</sup> Therefore, the development of prion-like  $\alpha$ -synuclein in the context of the rapid Krabbe disease course of 4–10 months in the present study, suggests this process can occur in a more accelerated time period than previously thought. It is notable that  $\alpha$ -synuclein in Krabbe disease was labelled by the Syn-O2 and 5G4 antibodies, both of which can recognize early oligomeric forms of  $\alpha$ -synuclein aggregates, while no labelling was observed with pS129, which typically occurs on the outside of Lewy bodies and may thus represent a late modification in the natural history of Lewy bodies.<sup>11,12,23</sup> Therefore, one could speculate that  $\alpha$ -synuclein aggregates in Krabbe disease represent an early stage of  $\alpha$ -synuclein aggregation. In RT-QuIC analysis, we found that only the soluble fraction of Krabbe disease brain lysates was seed-competent while we previously reported both aqueous- and detergent-soluble fractions as seed-competent in the same assay with LBD lysates.<sup>9</sup> As soluble  $\alpha$ -synuclein probably precedes insoluble forms, this may further support the proposition that  $\alpha$ -synuclein aggregates in Krabbe disease are less mature compared to those in LBD, which may also explain the lack of Lewy bodies.

A limitation of the present study is the small numbers of cases available, which limits generalizability; however, we endeavoured to identify as many cases as possible for the present study, including contacting other brain banks across the world but were limited by the inherent lack of availability of suitable tissues. Nevertheless, given that seed-competent  $\alpha$ -synuclein has not previously been identified in paediatric populations, we feel the present findings are important and will hopefully increase interest in the study of autoptotic Krabbe disease tissue.

In summary, we report the presence of seed-competent  $\alpha$ -synuclein conformers in brain lysates from infants with Krabbe disease. This constitutes the first description to our knowledge of such pathology in paediatric populations, and provides novel insights into mechanisms that may contribute to the formation of Lewy bodies in LBD.

## Acknowledgements

This paper is dedicated to the memory of all the infants whose tissues were used in this study and their families for their generosity and selflessness in agreeing to donate brain tissue for research.

Tissue for controls, the DLB case and KD Cases 1 and 3 was obtained from Newcastle Brain Tissue Resource, a UK Human Tissue Authority approved brain tissue repository funded in part by a grant from the UK Medical Research Council (G0400074), by NIHR Newcastle Biomedical Research Centre awarded to the Newcastle upon Tyne NHS Foundation Trust and Newcastle University, and by a grant from the Alzheimer's Society and Alzheimer's Research UK as part of the Brains for Dementia Research Project. Tissue for KD Case 2 was obtained from the University of Maryland Brain Bank, USA, through the NIH NeuroBioBank, and KD Case 4 from the Medical University of Vienna, Austria.

## Funding

This study was funded by Alzheimer's Research UK Fellowship awarded to D.E. (ARUK-RF2018C-005). The work conducted by the El-Agnaf laboratory was supported by Qatar Biomedical Research Institute under the Internal Grant Program SF 2017-007. C.H. was funded by South Tees Hospitals NHS Foundation Trust. D.K. is funded by The Lewy Body Society (LBS/007/2020). T.F.O. is supported by the Deutsche Forschungsgemeinschaft (DFG, German Research Foundation) under Germany's Excellence Strategy - EXC 2067/1-390729940 and by SFB1286 (B8). W.H. is supported by the NIHR GOSH BRC. The views expressed are those of the author(s) and not necessarily those of the NHS, the NIHR or the Department of Health.

## Competing interests

The authors declare no competing interests.

## Supplementary material

Supplementary material is available at *Brain* online.

## Appendix 1

Full details are provided in the [Supplementary material](#).

### International DLB Genetics Consortium members

USA: Jose Bras, Rita Guerreiro, Celia Kun-Rodrigues, Andrew Singleton, Dena Hernandez, Owen A. Ross, Dennis W. Dickson, Neill Graff-Radford, Tanis J. Ferman, Ronald C. Petersen, Brad F. Boeve, Michael G. Heckman, John Q. Trojanowski, Viviana Van Deerlin, Nigel J. Cairns, John C. Morris, David J. Stone, John D. Eicher, Lorraine Clark, Lawrence S Honig, Karen Marder, Geidy E. Serrano, Thomas G. Beach, Douglas Galasko, Eliezer Masliah.

UK: John Hardy, Lee Darwent, Olaf Ansorge, Laura Parkkinen, Kevin Morgan, Kristelle Brown, Anne Braae, Imelda Barber, Claire Troakes, Safa Al-Sarraj, Tom Warner, Tammaryn Lashley, Janice Holton, Yaroslau Compta, Tamas Revesz, Andrew Lees, Henrik Zetterberg, Valentina Escott-Price, Stuart Pickering-Brown, David Mann, Peter St. George-Hyslop.

Canada: Ekaterina Rogaeva, Peter St. George-Hyslop.

Spain: Jordi Clarimon, Alberto Lleo, Estrella Morenas-Rodriguez, Pau Pastor, Monica Diez-Fairen, Miquel Aquilar, Yaroslau Compta.

Australia: Claire Shepherd, Glenda M. Halliday.

Finland: Pentti J. Tienari, Liisa Myllykangas, Minna Oinas.

Portugal: Isabel Santana.

France: Suzanne Lesage.



Sweden: Henrik Zetterberg, Elisabet Londos.  
The Netherlands: Afina Lemstra.

## References

1. Graziano AC, Cardile V. History, genetic, and recent advances on Krabbe disease. *Gene*. 2015;555(1):2–13.
2. Outeiro TF, Koss DJ, Erskine D, et al. Dementia with Lewy bodies: An update and outlook. *Mol Neurodegener*. 2019;14(1):5.
3. Chang D, Nalls MA, Hallgrimsdottir IB, et al. A meta-analysis of genome-wide association studies identifies 17 new Parkinson's disease risk loci. *Nat Genet*. 2017;49(10):1511–1516.
4. Abdelkarim H, Marshall MS, Scesa G, et al.  $\alpha$ -Synuclein interacts directly but reversibly with psychosine: Implications for  $\alpha$ -synucleinopathies. *Sci Rep*. 2018;8(1):12462.
5. Marshall MS, Issa Y, Heller G, Nguyen D, Bongarzone ER. AAV-Mediated GALC gene therapy rescues alpha-synucleinopathy in the spinal cord of a leukodystrophic lysosomal storage disease mouse model. *Front Cell Neurosci*. 2020;14:619712.
6. Smith BR, Santos MB, Marshall MS, et al. Neuronal inclusions of  $\alpha$ -synuclein contribute to the pathogenesis of Krabbe disease. *J Pathol*. 2014;232(5):509–521.
7. Erskine D, Koss D, Korolchuk VI, et al. Lipids, lysosomes and mitochondria: Insights into Lewy body formation from rare monogenic disorders. *Acta Neuropathol*. 2021;141(4):511–526.
8. Erskine D, Attems J. Insights into Lewy body disease from rare neurometabolic disorders. *J Neural Transm (Vienna)* 2021;128(10):1567–1575.
9. Poggiolini I, Erskine D, Vaikath NN, et al. RT-QuIC using C-terminally truncated  $\alpha$ -synuclein forms detects differences in seeding propensity of different brain regions from synucleinopathies. *Biomolecules*. 2021;11(6):820.
10. Han JY, Jang HS, Green AJE, Choi YP. RT-QuIC-based detection of alpha-synuclein seeding activity in brains of dementia with Lewy body patients and of a transgenic mouse model of synucleinopathy. *Prion*. 2020;14(1):88–94.
11. Kumar ST, Jagannath S, Francois C, Vanderstichele H, Stoops E, Lashuel HA. How specific are the conformation-specific  $\alpha$ -synuclein antibodies? Characterization and validation of 16  $\alpha$ -synuclein conformation-specific antibodies using well-characterized preparations of  $\alpha$ -synuclein monomers, fibrils and oligomers with distinct structures and morphology. *Neurobiol Dis*. 2020;146:105086.
12. Vaikath NN, Majbour NK, Paleologou KE, et al. Generation and characterization of novel conformation-specific monoclonal antibodies for  $\alpha$ -synuclein pathology. *Neurobiol Dis*. 2015;79:81–99.
13. Raghavan R, Kruijff L, Sterrenburg MD, Rogers Beverly B., Hladik Christa L., White Charles L. Alpha-synuclein expression in the developing human brain. *Pediatr Dev Pathol*. 2004;7(5):506–516.
14. Orme T, Hernandez D, Ross OA, et al. Analysis of neurodegenerative disease-causing genes in dementia with Lewy bodies. *Acta Neuropathol Commun*. 2020;8(1):5.
15. Guerreiro R, Ross OA, Kun-Rodrigues C, et al. Investigating the genetic architecture of dementia with Lewy bodies: A two-stage genome-wide association study. *Lancet Neurol*. 2018;17(1):64–74.
16. Edison P, Rowe CC, Rinne JO, et al. Amyloid load in Parkinson's disease dementia and Lewy body dementia measured with [11C]PIB positron emission tomography. *J Neurol Neurosurg Psychiatry*. 2008;79(12):1331–1338.
17. Walker L, Stefanis L, Attems J. Clinical and neuropathological differences between Parkinson's disease, Parkinson's disease dementia and dementia with Lewy bodies - Current issues and future directions. *J Neurochem*. 2019;150(5):467–474.
18. Van Den Berge N, Ferreira N, Mikkelsen TW, et al. Ageing promotes pathological alpha-synuclein propagation and autonomic dysfunction in wild-type rats. *Brain*. 2021;144(6):1853–1868.
19. Marshall MS, Jakubauskas B, Bogue W, et al. Analysis of age-related changes in psychosine metabolism in the human brain. *PLoS ONE*. 2018;13(2):e0193438.
20. Durcan R, Wiblin L, Lawson RA, et al. Prevalence and duration of non-motor symptoms in prodromal Parkinson's disease. *Eur J Neurol*. 2019;26(7):979–985.
21. Stokholm MG, Danielsen EH, Hamilton-Dutoit SJ, Borghammer P. Pathological  $\alpha$ -synuclein in gastrointestinal tissues from prodromal Parkinson disease patients. *Ann Neurol*. 2016;79(6):940–949.
22. Kempster PA, O'Sullivan SS, Holton JL, Revesz T, Lees AJ. Relationships between age and late progression of Parkinson's disease: A clinico-pathological study. *Brain*. 2010;133:1755–1762.
23. Shahmoradian SH, Lewis AJ, Genoud C, et al. Lewy pathology in Parkinson's disease consists of crowded organelles and lipid membranes. *Nat Neurosci*. 2019;22(7):1099–1109.